APPLIED AND ENVIRONMENTAL MICROBIOLOGY, NOV. 1997, p. 4435–4440 Vol. 63, No. 11
0099-2240/97/$04.00 + 0
Copyright © 1997, American Society for Microbiology

Evidence That *Ceriporiopsis subvermispora* Degrades Nonphenolic Lignin Structures by a One-Electron-Oxidation Mechanism

EWALD SREBOTNIK,† KENNETH A. JENSEN, JR., SHINGO KAWAI,‡ AND KENNETH E. HAMMEL*

Institute for Microbial and Biochemical Technology, USDA Forest Products Laboratory, Madison, Wisconsin 53705

Received 9 July 1997/Accepted 29 August 1997

The white-rot fungus *Ceriporiopsis subvermispora* is able to degrade nonphenolic lignin structures but appears to lack lignin peroxidase (LiP), which is generally thought to be responsible for these reactions. It is well established that LiP-producing fungi such as *Phanerochaete chrysosporium* degrade nonphenolic lignin via one-electron oxidation of its aromatic moieties, but little is known about ligninolytic mechanisms in apparent nonproducers of LiP such as *C. subvermispora.* To address this question, *C. subvermispora* and *P. chrysosporium* were grown on cellulose blocks and given two high-molecular-weight, polyethylene glycol-linked model compounds that represent the major nonphenolic arylglycerol-β-aryl ether structure of lignin. The model compounds were designed so that their cleavage via one-electron oxidation would leave diagnostic fragments attached to the polyethylene glycol. One model compound was labeled with ^{13}C at C_α of its propyl side chain and carried ring alkoxyl substituents that favor C_α-C_β cleavage after one-electron oxidation. The other model compound was labeled with ^{13}C at C_β of its propyl side chain and carried ring alkoxyl substituents that favor C_β-*O*-aryl cleavage after one-electron oxidation. To assess fungal degradation of the models, the high-molecular-weight metabolizes derived from them were recovered from the cultures and analyzed by ^{13}C nuclear magnetic resonance spectrometry. The results showed that both *C. subvermispora* and *P. chrysosporium* degraded the models by routes indicative of one-electron oxidation. Therefore, the ligninolytic mechanisms of these two fungi are similar. *C. subvermispora* might use a cryptic Lip to catalyze these C_α-C_β and C_β-*O*-aryl cleavage reactions, but the data are also consistent with the involvement of some other one-electron oxidant.

The aromatic biopolymer lignin resists biodegradation by most organisms because it is nonhydrolyzable and consists of randomly linked stereoirregular structures (1, 10, 16). However, some specialized wood decay basidiomycetes have developed ligninolytic mechanisms which take advantage of the fact that lignin is susceptible to oxidative attack. The best-characterized ligninolytic system is found in white-rot fungi, such as *Phanerochaete chrysosporium,* that produce extracellular lignin peroxidases (LiPs) that have the unusual ability to abstract an electron from the recalcitrant nonphenolic arylglycerol-β-aryl ether (β-*O*-4-linked) units that make up the bulk of lignin. This reaction results in the formation of transient lignin cation radicals, which undergo spontaneous C_α-C_β cleavage to give benzaldehydes, C_β-*O*-aryl cleavage to give phenylglycerols, and other less prominent degradative reactions (7, 16, 19). So far, no mechanism other than one-electron oxidation has been shown to provide a route for the biodegradation of nonphenolic lignin structures.

Therefore, it is interesting that many white-rot fungi have been reported to lack LiP activity (9, 21, 23, 26). Little is known about ligninolytic strategies in these apparent nonproducers of LiP, but at least one of them, *Ceriporiopsis subvermispora,* degrades nonphenolic lignin structures (27). Preliminary evidence from isotope-trapping experiments shows that this fungus produces benzylic fragments when it cleaves the principal, nonphenolic, β-*O*-4-linked structure of lignin (11). These products (benzyl alcohols, benzaldehydes, and benzoate esters) could indicate that *C. subvermispora* cleaves the lignin side chain between C_α and C_β, which would be characteristic of a cation radical mechanism. However, previous data (11) do not rule out the possibility that these benzylic products arc quantitatively insignificant or that they are merely secondary products from the intracellular modification of other, uncharacterized cleavage metabolites.

To address this problem, we have designed ^{13}C-labeled polyethylene glycol (PEG)-linked lignin model compounds in which diagnostic cleavage fragments remain attached to high-molecular-weight (high-MW) polymer after attack by ligninolytic fungi. This approach yields relatively stable products that are not susceptible to intracellular fungal metabolism. Analysis of these polymeric fungal metabolites by ^{13}C nuclear magnetic resonance (NMR) spectrometry shows that the extracellular ligninolytic reactions of *C. subvermispora* are the same as those of the LiP producer *P. chrysosporium.* That is, *C. subvermispora* probably degrades nonphenolic lignin by a one-electron-oxidation mechanism.

MATERIALS AND METHODS

Organisms and reagents. *C. subvermispora* FP-90031 and *P. chrysosporium* ATCC 24725 were obtained from the Center for Forest Mycology, USDA Forest Products Laboratory.

LiPs were produced in rotary-shaken liquid cultures of *P. chrysosporium* and fractionated by ion-exchange chromatography on quaternary aminoethyl Sepharose (Pharmacia) as described previously (17). The partially purified LiP fraction used in these experiments consisted predominantly of isozymes H1 and H2.

Chemicals, all of reagent grade, were obtained from Aldrich or Sigma unless otherwise indicated.

Synthesis of PEG-linked lignin models. An *erythro-threo* mixture of α-^{14}C-labeled model I (2.4×10^8 dpm $mmol^{-1}$ of attached dimer) was prepared as described previously (13).

A modification of the same procedure was used to prepare α-^{13}C-labeled model VI. [1-^{13}C]acetic acid (16.4 mmol, 99.1% isotope purity; Isotec) was

*Corresponding author. Phone: (608) 231-9528. Fax: (608) 231-9262, E-mail: kehammel@facstaff.wisc.edu.

†Permanent address: Institut für Biochemische Technologies und Mikrobiologie, Technische Universität Wien, A-1060 Vienna, Austria.

‡ Permanent address: Department of Applied Bioorganic Chemistry, Gifu University, Gifu 501-11, Japan.

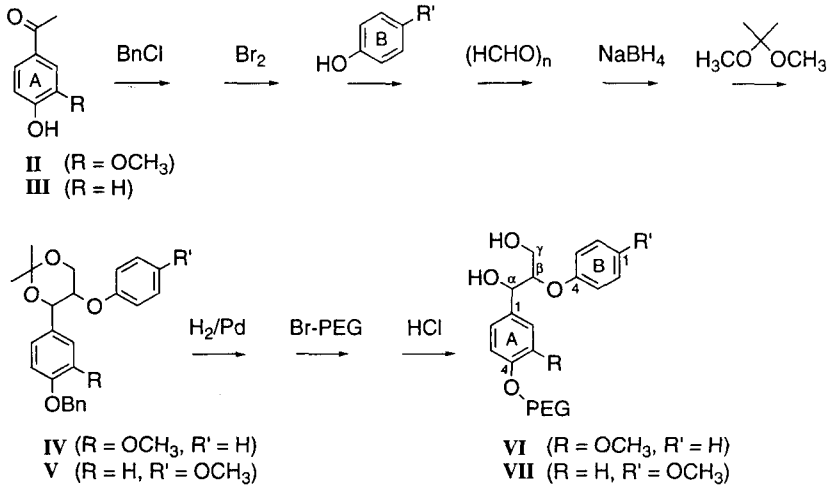

FIG. 1. Strategy for the synthesis of PEG-linked lignin models VI and VII. See Materials and Methods and reference 13 for details. Bn, benzyl; Br-PEG, brominated PEG.

condensed with guaiacol (19.7 mmol) to give 10.4 mmol of [α-^{13}C]acetovanillone (compound II). The synthetic procedure outlined in Fig. 1 was then used to convert compound II to 1.7 mmol of the acetonide-protected β-*O*-4-linked dimer IV. Compound IV consisted of a 1:1 *erythro-threo* mixture, which was resolved by column chromatography on silica gel 60 in hexane-ethyl acetate (3:1). The *erythro* isomer was then debenzylated at position 4 of its A ring, reacted with brominated PEG (8,000 MW), and deprotected at its α and γ positions to give model VI (2.4 g of polymer with 0.47 mmol of attached dimer). The same approach was used to prepare α-^{14}C-labeled model VI from (l-^{14}C]acetic acid (Sigma) and unlabeled precursors. A small quantity of the ^{14}C-labeled model was added to the ^{13}C-labeled model (final specific activity, 4.4×10^6 dpm mmol^{-1} of attached dimer) to assist with mass balance determinations during the biodegradation experiments. Table 1 shows ^{13}C NMR structure assignments for a natural-abundance preparation of model VI.

The same approach was used to prepare β-^{13}C-labeled model VII. [2-^{13}C]acetic acid (16.7 mmol, 99.0% isotope purity; Isotec) was condensed with phenol (50.1 mmol) to give 16.6 mmol of labeled *p*-hydroxyacetophenone (compound III). The synthetic procedure outlined in Fig. 1 was then used to convert compound III to 3.1 mmol of the acetonide-protected β-*O*-4 dimer V. Compound V consisted of a 3:1 *erythro-threo* mixture, which was resolved by column chromatography on Silica Gel 60 in benzene-methanol (200:1). The *erythro* isomer was then debenzylated at position 4 of its A ring, reacted with brominated PEG (8,000 MW), and deprotected at its α and γ positions to, give model VII (5.6 g of polymer with 0.55 mmol of attached dimer). The foregoing procedure was also used to prepare β-^{14}C-labeled model VII from [2-^{14}C]acetic acid (Sigma) and unlabeled precursors. A small quantity of the ^{14}C-labeled model was added to the ^{13}C-labeled model (final specific activity, 8.1×10^7 dpm mmol^{-1} of attached dimer) to assist with mass balance determinations during the biodegradation experiments. Table 1 shows ^{13}C NMR structure assignments for a natural-abundance preparation of model VII.

TABLE 1. ^{13}C NMR signal assignments for models VI and VII

Chemical shift of compound (δ, ppm)[a]		Assignment[b]
Model VI	Model VII	
55.8	55.6	—OCH_3
61.3	61.7	—$C_\gamma H_2OH$
61.5	61.2	—OCH_2CH_2OH of PEG
68.6	67.4	—OCH_2CH_2OAr of PEG
69.5	69.7	—OCH_2CH_2OAr of PEG
70.5	70.5	Internal —OCH_2CH_2O— of PEG
72.5	72.0	—OCH_2CH_2OH of PEG
73.6	72.5	—$C_\alpha HOH$—
82.0	83.4	—$C_\beta OHAr$—
110.6		A2
113.5		A5
	114.4	A3 and A5, or B2 and B6
	114.6	A3 and A5, or B2 and B6
116.3	118.3	B3 and B5
118.9		A6
121.1		B1
	127.6	A2 and A6
129.4		B2 and B6
135.0	133.4	A1
147.5		A3 or A4
149.3		A3 or A4
	151.9	B4
	154.5	B1
158.1		B4
	158.3	A4

[a] Chemical shifts are relative to tetramethylsilane in $CDCl_3$.
[b] The carbon responsible for each NMR signal is shown in boldface type. See Fig. 1 for labeling of chemical structures.

Fungal degradation of PEG-linked models. The substrate for solid-state cultures was prepared from sheets of cellulose (Lenzing AG, Lenzing, Austria). This material is a highly bleached wood pulp normally used as a feedstock for viscose manufacture. The sheets were cut to dimensions of 2 by 2 by 0.2 cm and shaken gently in water to loosen the fiber structure. For each culture, five cellulose sheets were stacked and dried overnight under a vacuum at 70°C to give a block with a dry weight of 2 g. The cellulose blocks were autoclaved and dried again under a vacuum in a sterile desiccator jar, and replicate blocks were infused with 1.3 ml of PEG-linked lignin model compound solution in methanol. The amounts of polymer added to each culture were 16 mg (3.3×10^5 dpm) for model I, 23 mg (2.0×10^4 dpm) for model VI, and 27 mg (2.1×10^5 dpm) for model VII. After evaporation of the methanol under reduced pressure in a sterile desiccator jar, the blocks were infused with 1.6 ml of fungal inoculum in basal low-nitrogen medium that contained 0.1% glucose and 10 mM sodium 2.2-dimethylsuccinate buffer (15). The *C. subvermispora* inoculum was buffered at pH 5.0 and consisted of a blended mycelial suspension. The *P. chrysosporium* inoculum was buffered at pH 4.5 and consisted of a conidiospore suspension.

The inoculated cellulose blocks (five or six replicates of each type) were placed on Teflon spacers over 2% water agar in 125-ml Erlenmeyer flasks. The flasks were fitted with gassing manifolds and incubated at 29°C *(C. subvermispora)* or 39°C *(P. chrysosporium).* After 3 days of incubation and *every* 2 days thereafter, the flask headspaces were flushed with sterile air, and vented $^{14}CO_2$ was trapped in an alkaline scintillation cocktail (14) to determine how much lignin model compound was mineralized.

To check the *C. subvermispora* cultures for possible contamination by *P.* chrysosporium, we took advantage of the fact that the latter fungus grows rapidly at 39°C, whereas the former is not viable at this temperature. At the conclusion of each biodegradation experiment, one block was removed from its flask, portions of it were placed on potato dextrose agar in petri plates, and the plates were incubated at 29 or 39°C. Colonization of the agar occurred rapidly at both temperatures with blocks inoculated with *P. chrysosporium* but occurred only at 29°C with blocks inoculated with *C. subvermispora.* Moreover, the morphology of the mycelium subcultured from *C. subvermispora* cellulose block cultures was identical to that of the original inoculum and distinct from that of *P. chrysosporium.*

Culture workup. Cultures were harvested after 7 or 8 days for model I, 10 or 11 days for model VI. and 7 days for model VII. They were extracted with methanol-water (9:1) (model I) or water (models VI and VII) overnight on a rotary shaker at 200 rpm, after which 10 ml of *N,N*-dimethylformamide was added to each extract. The extracts were filtered, evaporated under reduced pressure to approximately 5 ml, centrifuged to remove insoluble material, and fractionated by gel permeation chromatography (GPC) on a column of Sephadex LH-20 (Pharmacia) (1.9 by 33 cm) in *N,N*-dimethylformamide. Fractions (1.5 ml) were collected, and an aliquot of each was assayed for ^{14}C by scintillation counting.

Analysis of low-MW products derived from model I. GPC fractions with elution volumes of between 61 and 80 ml were pooled, evaporated under reduced pressure, redissolved in 1.5 ml of methanol-water-formic acid (10:90:1), and filtered. Portions (0.25 ml) were then subjected to reversed-phase high-performance liquid chromatography (HPLC) on a C_{18} column (Vydac 201TP; 250 by 4.6 mm; 10-μm particle size). Metabolites were eluted at 1.0 ml min^{-1} and ambient temperature with a 10:90:1 mixture of methanol-water-formic acid for 5 min followed by a 39-min linear gradient to 62:38:1 methanol-water-formic acid. Fractions (0.5 ml) were collected, and an aliquot of each was analyzed for ^{14}C by scintillation counting.

Preliminary product identifications were made by comparing elution times with those of authentic standards. Collected peak fractions that contained each of the metabolites were then pooled, extracted with CH_2Cl_2, dried over Na_2SO_4, evaporated to dryness, trimethylsilylated, and identified by gas chromatography-electron impact mass spectrometry (GC-MS). In experiments with *C. subvermispora*, the identifications were also confirmed by converting the metabolites chemically to new products, which were then compared with authentic standards by reversed-phase HPLC. Compound X was oxidized to compound XI with 2,3-dichloro-5,6-dicyanobenzoquinone (DDQ) (11), compound XI was reduced to compound X with $NaBH_4$ (11), and compound IX was hydrolyzed to 4-ethoxy-3-methoxybenzoic acid with 10% NaOH (6).

Chemical and enzymatic conversions of models VI and VII. Model XVI was prepared by oxidizing model VII with a 2.5-fold molar excess of DDQ in CH_2Cl_2 overnight at ambient temperature. The solvent was then evaporated under a stream of argon, the residue was taken up in a 1:9 methanol-water mixture, and the resulting solution was applied to a solid-phase extraction column (Alltech Hi-load C_{18}). The column was rinsed with several volumes of l:9 methanol-water, after which the product, model XVI, was eluted with 7:3 methanol-water and purified by GPC as outlined above for the samples from fungal cultures.

Models VI, VII, and XVI were oxidized with LiP in the presence of H_2O_2 at ambient temperature. Typical reaction mixtures (30 ml) contained 0.5 mM PEG-linked lignin structure, 0.25 mM H_2O_2, 0.25 μM LiP, and 20 mM sodium glycolate (pH 4.5). Reactions were monitored spectrophotometrically at 308 nm (17), and the pH was adjusted to 6.5 to 7.0 with NaOH as soon as the absorbance change ceased (5 to 20 min). The samples were then purified by GPC as described above.

Chemical reductions of products from the LiP-catalyzed oxidation of models VI, VII, and XVI were carried out overnight with 0.1 M $NaBH_4$ in 95% ethanol at 4°C, after which excess reductant was destroyed with formic acid. Chemical oxidations of the reduced samples were carried out with DDQ as described above for model XVI. All of the chemically modified polymers were purified by GPC as described above.

^{13}C NMR analyses of polymeric products derived from models VI and VII. GPC fractions with elution volumes of between 35 and 45 ml were pooled and evaporated under reduced pressure. The residue (containing 6 to 9 μmol of lignin-related structures) was redissolved in approximately 0.5 ml of dimethyl-d_6 sulfoxide and transferred to a 5-mm-diameter NMR tube. ^{13}C NMR analyses were obtained at 62.9 MHz and 300 K on a Bruker DPX250 spectrometer with a Bruker QNP probe. Proton-decoupled ^{13}C spectra were acquired with a 30° pulse and a relaxation delay of 1.0 s for a total of at least 8×10^4 transients. The data consisting of 1.6×10^4 points, were zero filled to 3.2×10^4 points, and a line broadening of 2 Hz was applied before Fourier transformation. Chemical shifts were referenced by setting the central dimethyl-d_6 sulfoxide signal to 39.5 ppm.

RESULTS

Degradation of model I in solid-state cultures. Preliminary assessments of ligninolytic activity in cellulose block cultures were obtained with a ^{14}C-labeled β-*O*-4 model linked to PEG through its B ring (model I [Fig. 2]). Both fungi exhibited a lag of about 4 days before they mineralized model I, after which $^{14}CO_2$ evolution gradually increased to a rate of about 4% per day over the next few days and then gradually declined. These results are similar to what we found with model I in wood block cultures of *P. chrysosporium* and *C. subvermispora* (11, 13) and are also consistent with previous observations that the two fungi delignify wood at similar rates (22, 28).

As shown in Table 2, the *P. chrysosporium* cultures accumulated a large quantity of radiolabeled low-MW metabolites derived from the cleavage of ^{14}C-labeled model I. GPC of culture extracts showed that after 8 days, about one-third of the model I initially added was present as material with an MW of less than about 350. Reversed-phase HPLC and GC-MS analyses of the collected fractions showed that most of this low-MW material consisted of 4-ethoxy-3-methoxybenzyl alcohol (compound VIII), a product we previously observed in wood block cultures and liquid cultures of *P. chrysosporium* (13). The cultures also cleaved model I by a route we did not previously report: the *erythro* and *threo* isomers of 1-(4-ethoxy-3-methoxyphenyl)propane-1,2,3-triol (phenylglycerol X) were identified from their HPLC retention times and by GC-MS (Table 3 and Fig. 2). These results arc consistent with extensive earlier studies which showed that both *P. chrysosporium* and its purified LiPs accomplish the C_α-C_β cleavage and C_β-*O*-aryl cleavage of macromolecular β-*O*-4-linked lignin structures (7, 10, 16).

Low-MW cleavage products accumulated to a significantly

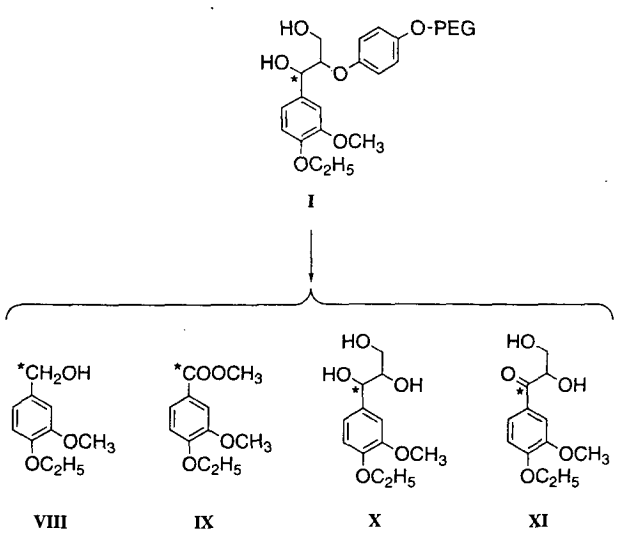

FIG. 2. Low-MW products obtained when model I was degraded by solid-state cultures of *P. chrysosporium* and *C. subvermispora*. The positions of the ^{14}C-labeled carbon are indicated (asterisks).

TABLE 2. Mass balances for model compound degradation in solid-state cultures of *P. chrysosporium* and *C. subvermispora*

Model compound	Fraction	Yield[a] (% of ^{14}C initially added to cultures)	
		P. chrysosporium	*C. subvermispora*
I	Mineralized	7[b]	8[c]
	Low MW	35[b]	13[c]
	High MW	43[b]	63[c]
VI	Mineralized	6[d]	6[e]
	Low MW	24[d]	17[e]
	High MW	59[d]	65[e]
VII	Mineralized	7[c]	8[c]
	Low MW	7[c]	10[c]
	High MW	65[c]	61[c]

[a] Missing ^{14}C consists of losses during workup and of unsoluble material.
[b] After 8 days.
[c] After 7 days.
[d] After 11 days.
[e] After 10 days.

TABLE 3. Product formation from fungal degradation of model I

Product	HPLC peak retention time (min)	Yield (% of ^{14}C initially added to cultures)		Mass spectrum[a] *m/z* (relative intensity)
		P. chrysosporium	*C. subvermispora*	
VIII	26.6	17.6	≤0.1[b]	254 (M^+, 90), 239 (4), 225 (13), 223 (14), 211 (16), 209 (22), 179 (9), 165 (100), 151 (2)
IX	41.0	≤0.1[c]	0.7	210 (M^+, 60), 182 (38), 179 (3), 151 (100)
X	12.2, 15.5[d]	5.6	5.8	458 (M^+, 1), 255 (4), 253 (100)
XI	23.0	≤0.6[c]	0.7	384 (M^+, 5), 369 (2), 268 (58), 253 (6), 205 (38), 204 (10), 179 (100), 151 (22)

[a] Mass spectra of trimethylsilyl derivatives.
[b] Chromatogram contained a mixture of minor unidentified products at this retention time. Product VIII was identified in the mixture by GC-MS.
[c] Chromatogram contained a mixture of minor unidentified products at this retention time. GC-MS analysis was not done.
[d] *erythro* and *threo* isomers (order of elution not determined).

lesser extent in the *C. subvermispora* cellulose block cultures after 7 days, even though mineralization was as rapid as it was in *P. chrysosporium* cultures (Table 2). HPLC analysis and GC-MS of the collected fractions showed that phenylglycerol X was the major low-MW product and that small quantities of l-(4-ethoxy-3-methoxyphenyl)-1-oxo-propane-2,3-diol (phenylketol XI) and 4-ethoxy-3-methoxybertzoic acid methyl ester (product IX) also accumulated (Table 3 and Fig. 2). These products are similar to those found in *P. chrysosporium,* but the low yields make it difficult to determine whether the reactions that lead to them are significant. Moreover, the data do not exclude the possibility that the metabolizes were produced intracellularly.

Design of models VI and VII. To address these problems, we attached (β-*O*-4-linked structures to PEG via their A rings, so that products from C_α-C_β cleavage and C_β-*O*-aryl cleavage would remain attached to high-MW polymer. Model VI was prepared with two electron-donating alkoxyl substituents on the A ring and only one on the B ring (Fig. 1), a configuration which favors C_α-C_β cleavage of the model VI cation radical (8). Model VII was prepared with only,one alkoxyl substituent on the A ring and two on the B ring (Fig. 1), which is expected to favor C_β-*O*-aryl cleavage of its cation radical (20). Both models were prepared with ^{13}C labels at positions adjacent to the cleavage site under investigation, model VI at C_α and model VII at C_β, so that functional-group changes could be detected by ^{13}C NMR spectrometry.

Oxidation of α-^{13}C-labeled model VI. Mass balances for the degradation of model VI by *P. chrysosporium* and C. *subvermispora* are shown in Table 2. ^{13}C NMR spectrometry of the high-MW fraction from culture extracts showed that C_α, in untreated controls exhibited a single prominent signal at 71.4 ppm (Fig. 3C), whereas the samples from fungal cultures contained additional signals at 191.4 and 195.0 ppm (Fig. 3A and B). These two signals were also produced when model VI was oxidized in vitro with LiP and H_2O_2 (data not shown). A distortionless enhancement with polarization transfer experiment showed that the 191.4-ppm signal was due to a carbon that carried a single hydrogen and that the 195.0-ppm signal was due to an unprotonated carbon (data not shown).

The 191.4-ppm chemical shift is characteristic of a benzylic aldehyde (structure XII) and therefore indicates C_α-C_β cleavage of model VI. The 195.0-ppm chemical shift is characteristic of a benzylic ketone and is therefore attributable to the uncleaved structure XIII (Fig. 3A and B and 4) (25). These results indicate oxidation of the model VI A ring and are consistent with earlier data on the LiP-catalyzed oxidation of β-*O*-4 dimers with this alkoxyl substitution pattern (8, 18, 20).

To check the structure assignments, the LiP-oxidized sample was reduced with $NaBH_4$. This treatment caused the 191.4- and 195.0-ppm signals to disappear and generated a new signal at 62.8 ppm (data not shown). The 62.8-ppm signal is characteristic of C_α in a benzyl alcohol (25) and therefore confirms that structure XII was a benzaldehyde. The reduced form of structure XIII was simply the starting material, structure VI, and consequently yielded no new signal.

Oxidation of β-^{13}C-labeled model VII. Mass balances for the degradation of model VII by *P. chrysosporium* and *C. subvermispora* are shown in Table 2. ^{13}C NMR spectrometry of the high-MW fractions from culture extracts showed that C_β in untreated controls exhibited a single prominent signal at 84.7 ppm (Fig. 3F), whereas samples from fungal cultures contained an additional major signal at 75.4 ppm, as well as smaller ones at 73.3, 74.3, 80.8, and 81.5 ppm (Fig. 3D and E). The 73.3-, 75.4-, and 80.8-ppm signals were also produced when model VII was oxidized in vitro with LiP and H_2O_2 (data not shown).

The 73.3-, 74.3-, and 75.4-ppm chemical shifts are characteristic of a —CH(OH)— group at C_β and therefore indicate cleavage of the β-*O*-4 linkage in model VII. The 80.8- and 81.5-ppm signals indicate uncleaved —CH(OAr)— structures that retain the original β-*O*-4 ether linkage (25).

To identify some of these structures, we subjected model VII to a series of chemical and enzymatic oxidoreductions. First, oxidation of the model with DDQ resulted in a shift of the $^{13}C_\beta$ NMR signal from 84.7 to 81.5 ppm, from which we conclude that this signal represents the ketone XVI. Next, oxidation of ketone XVI with LiP gave a single new signal at 74.3 ppm. Since previous work has shown that β-*O*-4-linked models with a ketone group at C_α undergo B-ring oxidation and β-*O*-aryl cleavage by LiP to give phenylketols (18), we conclude that the 74.3-ppm signal represents the phenylketol XV. Finally, reduction of phenylketol XV with $NaBH_4$ gave a single new signal at 75.4 ppm, from which we conclude that this signal represents the phenylglycerol XIV (Fig. 3D and E and 5). These results establish that phenylglycerol XIV was the major oxidation product formed from model VII by both *C. subvermispora* and *P. chrysosporium.*

The —C β H(OH)— structure responsible for the 73.3-ppm signal was not identified but probably contains a —C_αH(OH)— group, because the signal shifted upfield after oxidation with DDQ and then shifted back to 73.3 ppm after reduction of the DDQ-treated sample with $NaBH_4$ (data not shown). The —C_βH(OAr)— group responsible for the 80.8-ppm signal also remains unidentified but probably contains a —C_α (=O)— group, because the signal disappeared after reduction with $NaBH_4$ and then reappeared after oxidation of the $NaBH_4$-treated sample with DDQ (data not shown).

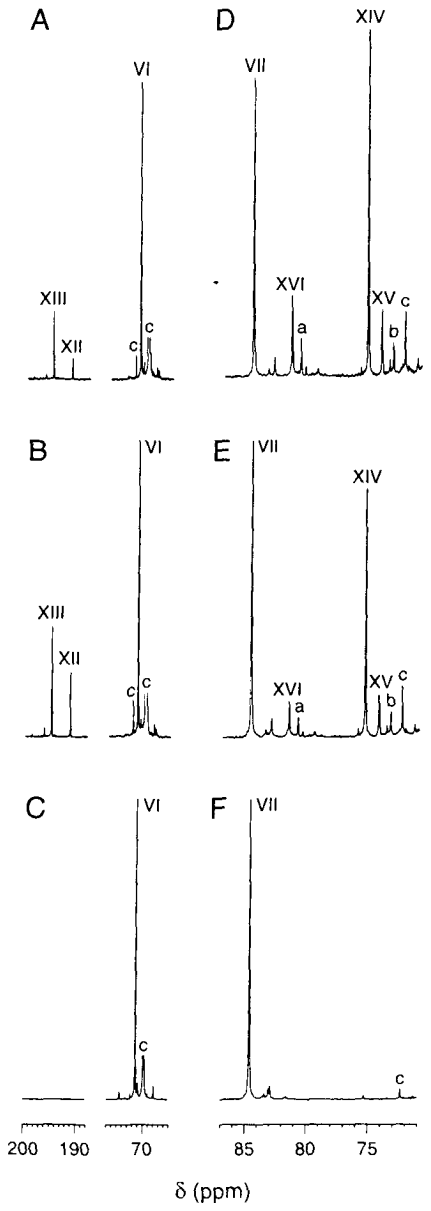

FIG. 3. ^{13}C NMR spectra of PEG-linked metabolites from models VI (A to C) and VII (D to F). Spectra A and D were obtained after degradation by *C. subvermispora*. Spectra B and E were obtained after degradation by *P. chrysosporium*. Spectra C and F were obtained from uninoculated controls. Structures which are shown in Fig. 4 and 5 (roman numerals), unidentified structures which are discussed in the text (a and b), and natural-abundance signals contributed by the PEG backbone (c) are labeled. In spectra A to C, the internal methylene PEG signal at 69 to 70 ppm has been truncated to simplify the figure, and the region from 77 to 188 ppm has been omitted because it contained no diagnostic signals. All of the spectra have been normalized by setting the starting material signal (VI or VII) to a constant height.

DISCUSSION

Previous work has shown that *P. chrysosporium* and *C. subvermispora* degrade lignin model compounds at similar rates in wood block cultures (27), which is consistent with observations that they delignify wood at similar rates (22, 28). In liquid medium. by contrast, *C. subvermispora* degrades lignin models at suboptimal rates, whereas *P. chrysosporium* degrades them at anomalously high rates (11, 13, 27). These observations led us to conclude that solid-state cultures would be better systems for initial tests of the new ^{13}C-labeled lignin models. However, we modified our previous solid-state culture system by using blocks of cellulose rather than wood as the growth substrate, because this approach avoided lignins and extractives that would interfere with product analyses.

Assessment of $^{14}CO_2$ evolution from ^{14}C-model I in the cellulose block cultures showed that they mineralized the model at about the same rate as wood block cultures and more rapidly than cultures in liquid medium (11). As we observed earlier for wood block cultures and liquid medium, the *P. chrysosporium* cellulose cultures accumulated significant quantities of the alcohol VIII, a benzylic product that suggests C_α-C_β cleavage of model I, whereas the *C. subvermispora* cultures did not (11). *C. subvermispora* does produce low levels of another benzylic product, the ester IX, in all three culture systems, but it degrades low-MW benzylic metabolizes rapidly and significant production is discernible only in isotope-trapping experiments (11). In cellulose blocks, both fungi produced the phenylpropanoid products X and XI from model I, but the yields were too low to determine whether C_β-*O*-aryl cleavage is a significant route for model I degradation,

These technical difficulties with model I were successfully addressed by changing the point of PEG attachment from the model's A ring to its B ring and by labeling selected carbons in the model with ^{13}C so that functional-group changes in the polymer could be analyzed by NMR spectrometry, The results show that C_α-C_β cleavage is a significant route for model VI degradation, that C_β-*O*-aryl cleavage is a significant route for model VII degradation, and that the ligninolytic reactions of *P. chrysosporium* and *C. subvermispora* are essentially the same in solid-state culture. The polymeric metabolites produced from models VI and VII are structurally analogous to the low-MW products from model I and are strongly diagnostic for a one-electron-oxidation mechanism (7, 16, 19).

There are two possible explanations for our findings. One is that *C. subvermispora* produces LiP in solid-state cultures. It is noteworthy in this regard that the *C. subvermispora* genome contains *lip*-like sequences, although it remains unclear whether these genes are ever expressed (24). We found no LiP activity in the cellulose block cultures employed for these experiments (data not shown), but assays for LiP are known to

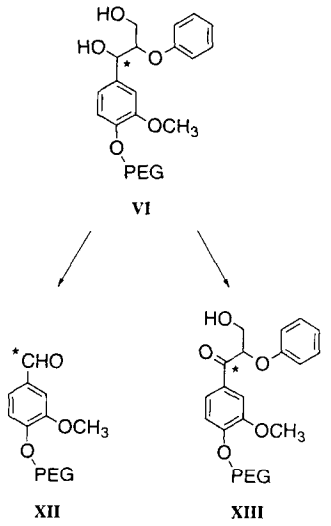

FIG. 4. Proposed routes for the oxidation of model VI by solid-state cultures of *P. chrysosporium* and *C. subvermispora*. Roman numerals refer to structures shown in Fig. 3A to C. The positions of the ^{13}C-labeled carbon are indicated (asterisks).

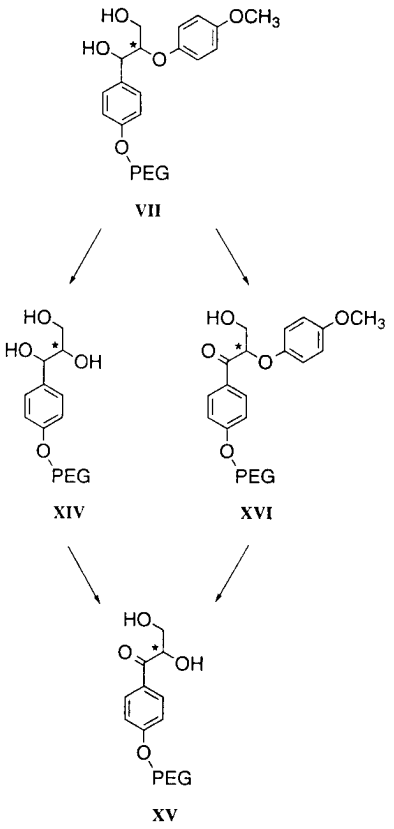

FIG. 5. Proposed routes for the oxidation of model VII by solid-state cultures of *P. chrysosporium* and *C. subvermispora*. Roman numerals refer to structures shown in Fig. 3D to F. The positions of the ^{13}C-labeled carbon are indicated (asterisks).

give unreliable results in solid-state culture extracts (4). To address this problem, we have begun efforts to replicate our ^{13}C NMR results with liquid cultures of *C. subvermispora,* in which LiP can be assayed reliably.

The alternative explanation is that *C. subvermispora* uses some other one-electron oxidant to cleave nonphenolic lignin structures. Several groups have proposed that enzymes other than LiP degrade lignin by working in concert with low-MW extracellular mediators (3, 5, 12). We recently showed that the manganese peroxidases of white-rot fungi promote lipid peroxidation reactions which accomplish the C_α-C_β cleavage and C_β-*O*-aryl cleavage of nonphenolic β-*O*-4-linked lignin structures (2, 11). This mechanism could provide a route for ligninolysis by *C. subvermispora,* which produces manganese peroxidases (26) and requires Mn to degrade lignin (11).

ACKNOWLEDGMENTS

We thank K. Hirth for the NMR analyses and R. Pettersen for the mass spectrometric analyses.

This work was supported by U.S. Department of Energy grant DE-FG02-94ER20140 (to K. E. H.) and by a fellowship (APART) from the Austrian Academy of Sciences (to E.S.).

REFERENCES

1. **Adler, E.** 1977. Lignin chemistry. Past, present and future. Wood Sci. Technol. **11:**169–218.
2. **Bao, W., Y. Fukushima, K. A. Jensen, Jr., M. A. Moen, and K. E. Hammel.** 1994. Oxidative degradation of non-phenolic lignin during lipid peroxidation by fungal manganese peroxidase. FEBS Lett. **354:**297–300.
3. **Bourbonnais, R., and M. Paice.** 1990. Oxidation of non-phenolic substrates: an expanded role for laccase in lignin biodegradation. FEBS Lett. **267:**99–102.
4. **Datta, A., A. Bettermann, and T. K. Kirk.** 1991. Identification of a specific manganese peroxidase among ligninolytic enzymes secreted by *Phanerochaete chrysosporium* during wood decay. Appl. Environ. Microbiol. **57:**1453–1460.
5. **Eggert, C., U. Temp, J. F. D. Dean, and K.-E. L. Eriksson.** 1996. A fungal metabolite mediates degradation of non-phenolic lignin structures and synthetic lignin by laccase. FEBS Lett. **391:**144–148.
6. **Furniss, B. S., A. J. Hannaford, P. W. G. Smith, and A. R. Tatchell (ed.).** 1989. Vogel's textbook of practical organic chemistry. John Wiley and Sons, New York, N.Y.
7. **Gold, M. H., H. Wariishi, and K. Valli.** 1989. Extracellular peroxidases involved in lignin degradation by the white rot basidiomycete *Phanerochaete chrysosporium*. Am. Chem. Soc. Symp. Ser. **389:**127–140.
8. **Hammel, K. E., M. D. Mozuch, K. A. Jensen, Jr., and P. J. Kersten.** 1994. H_2O_2 recycling during oxidation of the arylglycerol β-aryl ether lignin structure by lignin peroxidase and glyoxal oxidase. Biochemistry **33:**13349–13354.
9. **Hatakka, A.** 1994. Lignin-modifying enzymes from selected white-rot fungi: production and role in lignin degradation. FEMS Microbiol. Rev. **13:**125–135.
10. **Higuchi, T.** 1990. Lignin biochemistry: biosynthesis and biodegradation. Wood Sci. Technol. **24:**23–63.
11. **Jensen, K. A., Jr., W. Bao, S. Kawai, E. Srebotnik, and K. E. Hammel.** 1996. Manganese-dependent cleavage of nonphenolic lignin structures by *Ceriporiopsis subvermispora* in the absence of lignin peroxidase. Appl. Environ. Microbiol. **62:**3679–3686.
12. **Kapich, A. N., and L. N. Shishkina.** 1995. Linkage of lipid peroxidation and lignin degradation in the mycelium of xylotrophic basidiomycetes (hypothesis). Dokl. Akad. Nauk Belarusi **39:**63–66. (In Russian.)
13. **Kawai, S., K. A. Jensen, Jr., W. Bao, and K. E. Hammel.** 1995. New polymeric model substrates for the study of microbial ligninolysis. Appl. Environ. Microbiol. **61:**3407–3414.
14. **Kirk, T. K., W. J. Connors, R. D. Bleam, W. F. Hackett, and J. G. Zeikus.** 1975. Preparation and microbial decomposition of synthetic [^{14}C]lignins. Proc. Natl. Acad. Sci. USA **72:**2515–2519.
15. **Kirk, T. K., S. Croan, M. Tien, K. E. Murtagh, and R. L. Farrell.** 1986. Production of multiple ligninases by *Phanerochaete chrysosporium*: effect of selected growth conditions and use of a mutant strain. Enzyme Microb. Technol. **8:**27–32.
16. **Kirk, T. K., and R. L. Farrell.** 1987. Enzymatic "combustion": the microbial degradation of lignin. Annu. Rev. Microbiol. **41:**465–505.
17. **Kirk, T. K., M. Tien, P. J. Kersten, B. Kalyanaraman, K. E. Hammel, and R. L. Farrell.** 1990. Lignin peroxidase from fungi: *Phanerochaete chrysosporium*. Methods Enzymol. **188:**159–171.
18. **Kirk, T. K., M. Tien, P. J. Kersten, M. D. Mozuch, and B. Kalyanaraman.** 1986. Ligninase of *Phanerochaete chrysosporium*. Mechanism of its degradation of the non-phenolic arylglycerol β-aryl ether substructure of lignin. Biochem. J. **236:**279–287.
19. **Lundell, T., H. Schoemaker, A. Hatakka, and G. Brunow.** 1993. New mechanism of the C_α-C_β cleavage in non-phenolic arylglycerol β-aryl ether lignin substructures catalyzed by lignin peroxidase. Holzforschung **47:**219–224.
20. **Miki, K., V. Renganathan, and M. H. Gold.** 1986. Mechanism of β-aryl ether dimeric lignin model compound oxidation by lignin peroxidase of *Phanerochaete chrysosporium*. Biochemistry **25:**4790–4796.
21. **Orth, A. B., D. J. Royse, and M. Tien.** 1993. Ubiquity of lignin-degrading peroxidases among various wood-degrading fungi. Appl. Environ. Microbiol. **59:**4017–4023.
22. **Otjen, L., R. Blanchette, M. Effland, and G. Leatham.** 1987. Assessment of 30 white rot basidiomycetes for selective lignin degradation. Holzforschung **41:**343–349.
23. **Périé, F. H., and M. H. Gold.** 1991. Manganese regulation of manganese peroxidase expression and lignin degradation by the white rot fungus *Dichomitus squalens*. Appl. Environ. Microbiol. **57:**2240–2245.
24. **Rajakumar, S., J. Gaskell, D. Cullen, S. Lobos, E. Karahanian, and R. Vicuña.** 1996. *lip*-like genes in *Phanerochaete sordida* and *Ceriporiopsis subvermispora*, white-rot fungi from which lignin peroxidase has not been detected. Appl. Environ. Microbiol. **62:**2660–2663.
25. **Ralph, J., W. L. Landucci, S. A. Ralph, and L. L. Landucci.** 1993. NMR database of lignin and cell wall model compounds. 205th American Chemical Society National Meeting, 28 March to 2 April, Denver, Colo. Database available on the Internet at http://www.dfrc.wisc.edu or from the authors (e-mail: saralph@facstaff.wisc.edu).
26. **Rüttimann-Johnson, C., L. Salas, R. Vicuña, and T. K. Kirk.** 1993. Extracellular enzyme production and synthetic lignin mineralization by *Ceriporiopsis subvermispora*. Appl. Environ. Microbiol. **59:**1792–1797.
27. **Srebotnik, E., K. A. Jensen, Jr., and K. E. Hammel.** 1994. Fungal degradation of recalcitrant nonphenolic lignin structures without lignin peroxidase. Proc. Natl. Acad. Sci. USA **91:**12794–12797.
28. **Srebotnik, E., and K. Messner.** 1994. A simple method that uses differential staining and light microscopy to assess the selectivity of wood delignification by white rot fungi. Appl. Environ. Microbiol. **60:**1383–1386.